



Improved sensorless control with the ST62 MCU for universal motor

The universal motor is today the most widely used motor in home appliances (vacuum cleaner, washer, hand tool, food processor...). Three modes of operation exist:

- in many cases, it is directly connected to the mains, without any speed adjustment.

More and more, however, the decreasing cost of electronics allows to include an adjustable speed drive in the appliance. The control can be open loop or closed loop:

- in open loop mode, the speed is adjusted by the user but not regulated: it decreases when the load increases. This is the case in many vacuum cleaners for example.
- in closed loop mode, the speed is regulated. This mode is used when the speed must be accurately kept at a given value, in washers for example. This mode requires to add a speed sensor on the motor shaft. Such a sensor is usually a tacho generator or magnet sensor. The drawbacks of the speed sensor are many, but all boil down to higher cost and lower reliability, not to mention the extra bulk needed to accommodate the sensor inside the plastic housing of a drill for example.

This document describes a speed regulator without sensor: the speed sensing is performed indirectly by the ST6220, low-cost 8-bit microcontroller, measuring the motor current. Performance results are given, which are in line with the need of many home appliances.

1 UNIVERSAL MOTOR PRINCIPLES

The universal motor can be driven in AC or DC mode. Figure 1 shows the two most popular variable speed drive principles. The goal is to adjust the voltage seen by the motor in order to adjust its speed. In AC mode, the motor voltage is adjusted by varying the firing delay of a triac. This is done with a diac, resistor and capacitor when lowest cost is desired, and with an 8 bit micro-controller when higher performance and added features are desired, such as user interface or monitoring [1]. The switch is usually a triac, the cheapest power switch.

In DC mode, the motor is supplied by a high frequency pulse width modulated (PWM) DC voltage. The voltage seen by the motor is proportional to the PWM duty cycle, which can be adjusted to modify the speed. The power switch used to chop the DC voltage at high frequency is a power MOS or an IGBT. The DC mode has several advantages versus the AC mode (less acoustic noise, higher efficiency, lower harmonics content, all due to lower current ripple, as is shown in Figure 1). However, in low cost appliances, the AC mode still dominates due to its lower cost (no rectifier bridge, no fast diode, triac cheaper than IGBT or MOS). This is the mode we will focus on in the next pages.

The universal motor is a serial excitation motor. Therefore, the motoring torque is proportional to the square of the motor current: $T_m = k \cdot I^2$

The mechanical power is the product of the torque by the speed: $P = T_m \cdot \Omega$

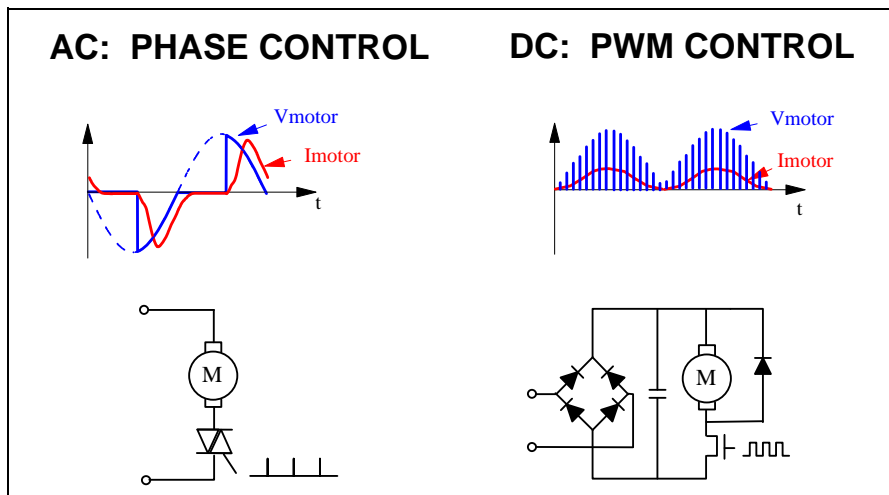
If we assume 100% efficiency, the mechanical power equals the electrical power $V \cdot I$ input to the motor. It follows that the speed is proportional to V/I :

$\Omega = k' \cdot V / I$ (V and I are *average* voltage and current over a mains period). The first consequence is that the motor speed is proportional to the average motor voltage.

At constant speed, the resistive torque T_r is equal to the motoring torque T_m . It comes from the previous equations that the speed is given by: $\Omega = k \cdot V / \sqrt{T_r}$.

This equation shows that when the resistive load torque increases at a given voltage, the motor speed will decrease, hence the need for speed regulation. This regulation can be performed by adjusting the average voltage V .

Figure 1. Universal motor variable speed drive: AC versus DC mode



2 SENSORLESS REGULATION PRINCIPLE

The above equations were first order equations, assuming DC operation, or average values for voltage and current. The real, instantaneous equation is the following:

While the triac is off:

$$i = 0$$

While the triac is on (after firing time t_d , and until current comes back to zero; see Figure 2):

$$v = e + z.i$$

with: e = back electromotive force (bemf) = $k. \Omega. i$

z = motor impedance = $r + j.L.\omega$

k = constant dependent upon motor characteristics

Ω = motor speed

i = instantaneous motor current

v = instantaneous motor voltage

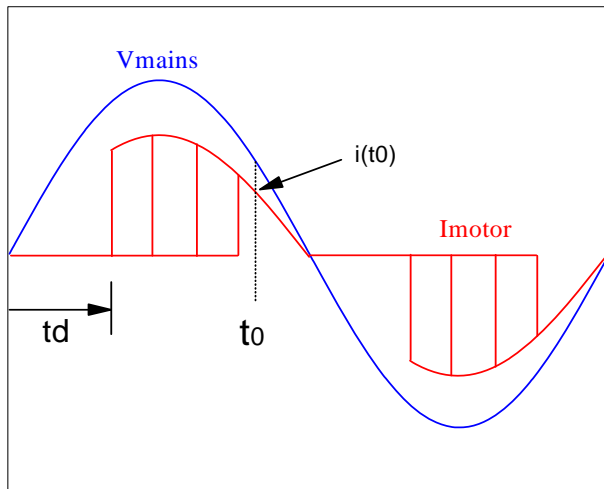
L = motor inductance

r = winding resistance

ω = mains frequency

$$v = (k.\Omega + r) i + j.L.\omega.i$$

Figure 2. First Order Model (resistive only): Constant Speed, Variable Load



In the time domain, $v(t)$ is the mains voltage: $v(t) = V_0 . \sin \omega t$ (V_0 = mains peak voltage).

At first order, we will neglect the inductive term $j.L.\omega$. This yields: $i(t) = k.\Omega + r$.

The universal motor behaves as a speed-dependent resistor of value $k.\Omega + r$.

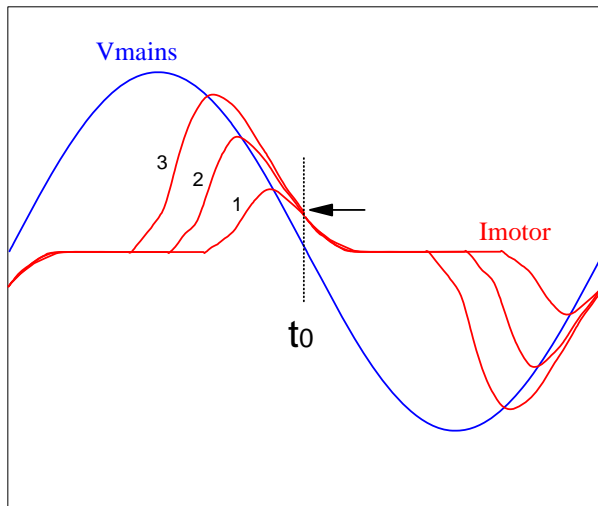
As Ω and r do not change very quickly, and v is known, measuring i at a specific time within the mains period (example: at time t_0 in Figure 2) gives an image of the motor speed: $\Omega = (V_0 / k. i(t_0)) \sin\omega t_0 - r / k$.

Therefore if we want to keep the speed at a fixed value Ω_0 , we need to keep $i(t_0)$ at a corresponding fixed value i_0 :

$$i_0 = V_0 . \sin\omega t_0 / (k.\Omega_0 + r)$$

In practice, each mains period, the micro-controller measures the current at time t_0 with its internal analog to digital converter. Then, the current error $i(t_0) - i_0$ is calculated, and the micro executes the speed regulation algorithm, which results in a new firing delay t_d . This delay is used to fire the triac on the next mains period. It is counted by the micro controller internal timer. The delay is measured starting from the mains voltage zero-crossing.

Figure 3. Measured Current in a Real Motor (resistive and inductive): Constant Speed, Variable Load (1: lowest load, 3: highest load)



If we now consider the real universal motor, including the inductive term $j.L.\omega$, we can apply the same method. Figure 3 shows the current and mains voltage for a real motor. On this figure, while the load is modified, the speed is kept constant by modi-

fying the triac firing delay. Moving from Figure 2 to Figure 3, we can see two effects of the inductive term. First effect: at triac turn-on, the motor current does not exhibit a discontinuity, but changes gradually from 0 to a finite value. Second effect: at mains voltage zero crossing, the motor current does not reach zero immediately, but keeps trailing for a few milliseconds. This trailing gives us more freedom to chose the measurement time t_0 . We can even chose the zero crossing instant, which is the easiest time for the micro-controller (no need to measure time t_0 with the timer, we can use the mains zero-crossing as an interrupt to the micro, which is necessary anyway for other matters). This is illustrated in Figure 3, where the arrow shows that the current is constant at the zero-crossing time while the motor load changes, provided that the speed is kept constant by adjustment of the firing delay t_d . For a detailed mathematical discussion, see annex 1.

To summarize, if we want to regulate the speed at a pre-defined set speed, for example 1000 rpm, we must measure the instantaneous motor current on every mains period at the same time t_0 (for example, on every mains voltage zero crossing following the positive half-cycle), and maintain this measured current at a fixed set current, 1 ampere for example. For a different set speed, 2000 rpm, we need to regulate the current around a different value, 0.5 ampere for example (note that a lower current corresponds to a higher speed).

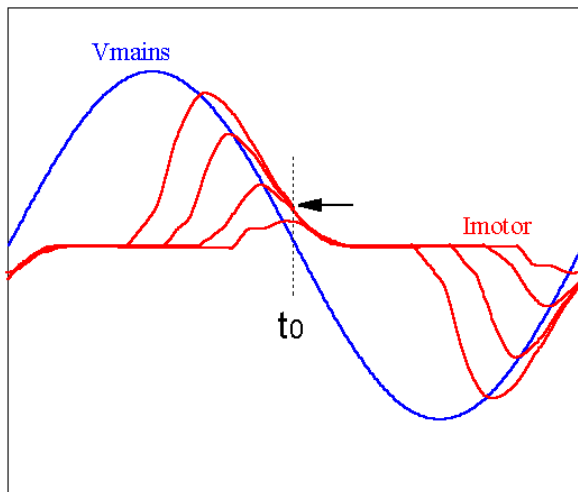
The regulation is performed by adjustment of the triac firing delay t_d .

The above described method gives very good results at medium and high speeds.

At very low speeds, we have a second order effect coming into the picture: Figure 4 is identical to Figure 3, except for the presence of a fourth current curve, corresponding to a very large firing delay t_d (this corresponds to a very low speed, combined with a low load). We can see on this fourth curve that the current at time t_0 is smaller than i_0 , current of the other 3 curves at this time. This effect is described in detail in annex 1. We have two solutions to cope with it. The simplest one is to limit the maximum firing delay (below values in the range of 7 mS, depending on the motor type). This means limiting the minimum speed which can be regulated. If the application cannot tolerate this reduction in its speed dynamic range, a second and more complex solution is to compensate this current measurement distortion, by means of look-up tables memorized in the micro-controller memory. When the current $i(t_0)$ is measured, if t_d is larger than a limit value (7 mS for example), $i(t_0)$ is increased by a compensation value extracted from a memory table before it is used to calculate the current error. This value is a function of the triac firing delay t_d , and is determined experimentally by characterizing the motor. The regulation system is not very sensitive to this value, so it is enough to characterize one motor of a given type, it is not neces-

sary to characterize each individual motor. Annex 2 describes how to determine this compensation table.

Figure 4. Measured Current at Constant Speed (for very large firing delays, current at time t_0 is lower than set current)



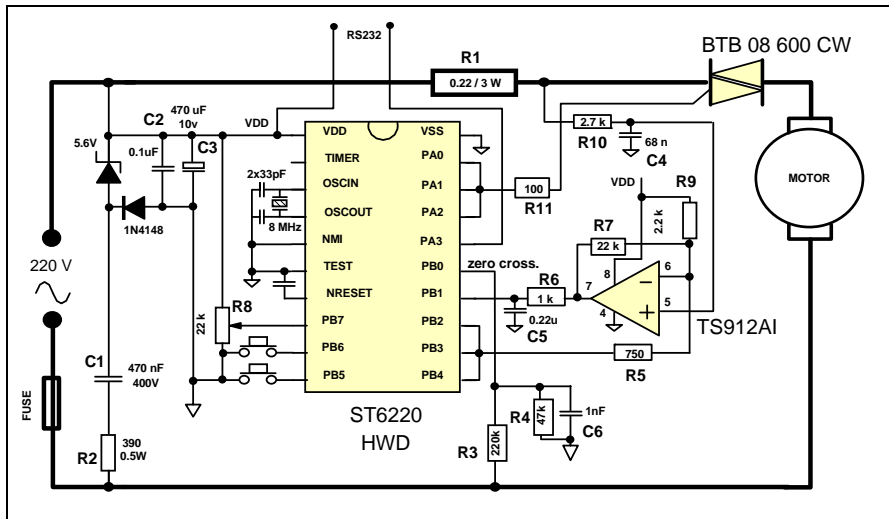
3 IMPLEMENTATION

Figure 5 gives a schematic of the sensorless motor drive. The heart of the system is the micro-controller, the ST6220, a low cost 8-bit general purpose micro. It is supplied directly from the mains by the capacitive supply made of components R2/C1/C2/C3 and of the two diodes. This is made possible by its low current consumption, in the range of 4 mA. This capacitive supply must be dimensioned to supply the micro, the operational amplifier, and the triac gate during the firing. Resistor R1 is the current sense resistor, it is only 0.22 ohm in order to keep the losses as low as possible (in this example, the motor is a 500 watts type). For this reason, an operational amplifier is needed in order to provide the micro-controller analog-to-digital converter input (pin PB1) with a large enough voltage. As this analog-to-digital converter (ADC) is an 8 bit type, its resolution (minimum voltage step discernible at its input) is around 20 mV when the micro is supplied from 5 volts. The larger the voltage on the ADC input, which is the op-amp output after some noise filtering by R6 and C5, the better the resolution on measured current $i(t_0)$, which will be used latter in the speed regulation algorithm. A value around 1 volt is a reasonable compromise. The op-amp must be a rail-to-rail type, at the output and inputs as well: for the input, the voltage measured on the sense resistor is very low, and referred to the positive supply VDD. The output should be able to swing from the micro-controller ground level to its VDD level, which are the same as for the op-amp itself, in order to make full usage of the ADC dynamic range.

Two noise filters (R10/C4 and R6/C5) are provided to remove brush noise from the motor current signal, before it is measured by the internal ADC. Depending on the motor, and with careful design, it is possible to do with only one filter.

Resistors R3, R4 and capacitor C6 are used to shape the mains voltage before sending it to the micro input pin PB0. This digital signal, which shows an edge at each zero-crossing of the mains (positive or negative edge depending on the half-cycle sign), interrupts the micro-controller program to signal the zero-crossing. It is used to synchronize the triac firing with the mains, and to trigger the ADC reading in order to acquire the current value $i(t_0)$.

Figure 5. A low cost 8-bit micro-controller ST6220, a rail-to-rail operational amplifier TS912, a triac and a small value sense resistor make the heart of this sensorless speed regulated drive



The triac is controlled by pins PA0/PA1/PA2 of the micro. They are in parallel in order to get enough current to trigger the triac. The 100 ohm resistor R11 limits the current in the triac gate.

Two push-buttons are provided on pins PB5 and PB6 of the micro for the user interface. Pushing one speeds up the motor, pushing the other slows it down. Alternatively, it is possible to replace this push-button interface by a potentiometer R8, which could be measured by the internal ADC. Both are shown on Figure 5, buttons and potentiometer, but the attached software only implements the push-buttons.

Finally, Figure 5 shows an output of the micro-controller labeled RS232 (together with the VDD supply). In the attached software, some routines are provided to help in the application development and motor characterization. They allow to connect the motor control board to the serial port COM1 of a personal computer. While the motor is running, the personal computer displays in a graphical form motor data such as measured current and firing delay, allowing easy interpretation and measurement. Of course, it is necessary to use opto-isolated components to connect the computer to the motor drive. This connection to a personal computer is described in annex 3.

4 SOFTWARE DESCRIPTION

Figure 6 illustrates the micro-controller program operation. The program consists of a loop synchronized on the mains zero-crossing (z.c.). Each zero-crossing causes an interrupt on pin PBO of the micro. In case of a positive half-cycle, the motor current $i(t_0)$ is measured and saved into variable it_0 for latter use. Then, in both cases (positive and negative half-cycle), the micro uses the timer to wait an amount of time $td \times 48 \mu S$, after which it fires the triac with pins PA0, PA1, PA2 ($48 \mu S$ is the chosen timer step). Three pins are used in order to supply up to $3 \times 20mA$ to the triac gate. The timer is used again to keep the gate activated during $400 \mu S$ ($TGATE \times 48 \mu S$). After the end of the triac gate activation, two tasks remain to accomplish: in the positive half-cycle, the micro reads the push-buttons (or potentiometer) to check the user speed demand; in the negative half-cycle, the regulation algorithm is executed, resulting in the calculation of a new value for td , to be applied on next mains cycle. When this is done, the micro returns to wait mode until the next zero-crossing interrupt happens.

•Regulation algorithm: proportional-integral regulation

This algorithm is contained within the subroutines “regul” and “pi”. Its input is the variable it_0 (current measured at zero-crossing), and its output the triac firing delay td (each unit corresponds to $48 \mu S$ delay). The variable it_0 is first increased by a compensation value extracted from a memory table before it is used to calculate the current error. This value is a function of the triac firing delay td . The current error, i_err , is then obtained by subtracting the current demand $icalc0$, which depends only upon the user speed demand. The micro then calculates the proportional and integral terms of the proportional-integral algorithm: they are simply the current error i_err multiplied by constants (K_P and K_I). In the attached example, $K_P = 1/4$ and $K_I = 1/32$, but these coefficients must be adjusted for a given motor type. They dictate the transient behavior of the regulation. As there is no multiplication instruction in ST6 micro controllers, it is chosen to multiply or divide only by powers of two ($1/4$, $1/32$, $1/8$...) as this is fast and easy to perform by software. Subroutines for multiplication by $1/4$, $1/8$, $1/16$, $1/32$, $1/64$ are given in the program. In practice, this restriction is not a problem, as the transient performance is not very sensitive to these coefficients.

If we note with index (n) the variables related to the nth mains cycle, the complete PI (proportional-integral) algorithm can be expressed by:

$$i_err(n) = it0(n-1) + table(td(n-1)) - icalc0$$

$$sum(n) = sum(n-1) + KI * i_err(n)$$

$$td(n) = VITMIN - [sum(n) + KP * i_err(n)]$$

table(td(n-1)) is the current compensation coefficient extracted from the table, and associated to the corresponding value of the firing delay td, td(n-1).

sum(n) is the integral term, and $KP * i_err(n)$ the proportional term. VITMIN is a constant equal to the maximum firing delay ($150 \times 48 \mu S = 7.2 \text{ mS}$ in the example).

This is expressed in the program by:

```
i_err <- it0 + table(td) - icalc0
```

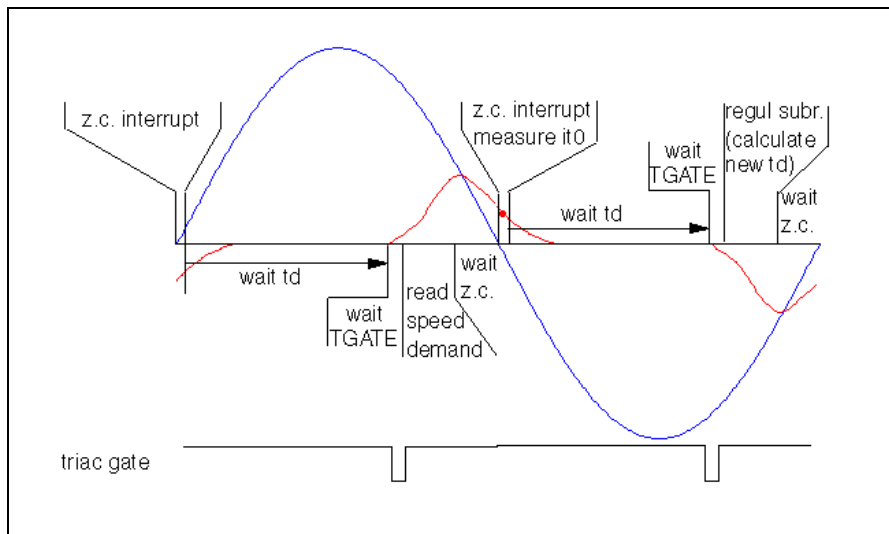
```
sum <- sum_old + KI * i_err
```

```
temp1 <- sum + KP * i_err
```

```
td <- VITMIN - temp1
```

```
sum_old <- sum
```

Figure 6. The program is a loop synchronized on the mains zero crossing (z.c.). It is identical on both half-cycles, except for the $i(t_0)$ current measurement, regulation subroutine and speed demand subroutine



The adaptation of the program to a specific motor type can be done by adjusting the coefficients K_I and K_P , and the contents of compensation table $table(td)$. The table is necessary only for the largest firing delays (slow speed). The slower the motor should be able to run, the more attention should be given to the elaboration of this table.

The proportional coefficient K_P adjusts how strongly the system reacts to a speed error: the larger this coefficient, the faster the reaction to load change, but if this term becomes too large, some instability may occur. The integral coefficient K_I adjusts the transient settling time when the load changes: the larger K_I , the faster the settling time, but again, instability may occur if this coefficient becomes too large. Trial and error is the best way to find the best compromises.

The latest detail which must be mentioned in the program is the operational amplifier gain adjust. At high speed, current $i(t_0)$ becomes very small; if we want to measure it with a reasonable accuracy, we must amplify it even more than in case of low speed. This is why the op-amp is fitted with a dual gain scheme, with help of resistor R_5 , connected to VDD or left open by the micro pins PB2/PB3/PB4. The op-amp gain is set to 10 for the low speed range, 40 for the high speed range. This gain setting is managed in subroutine "speed", which also checks for user speed demand.

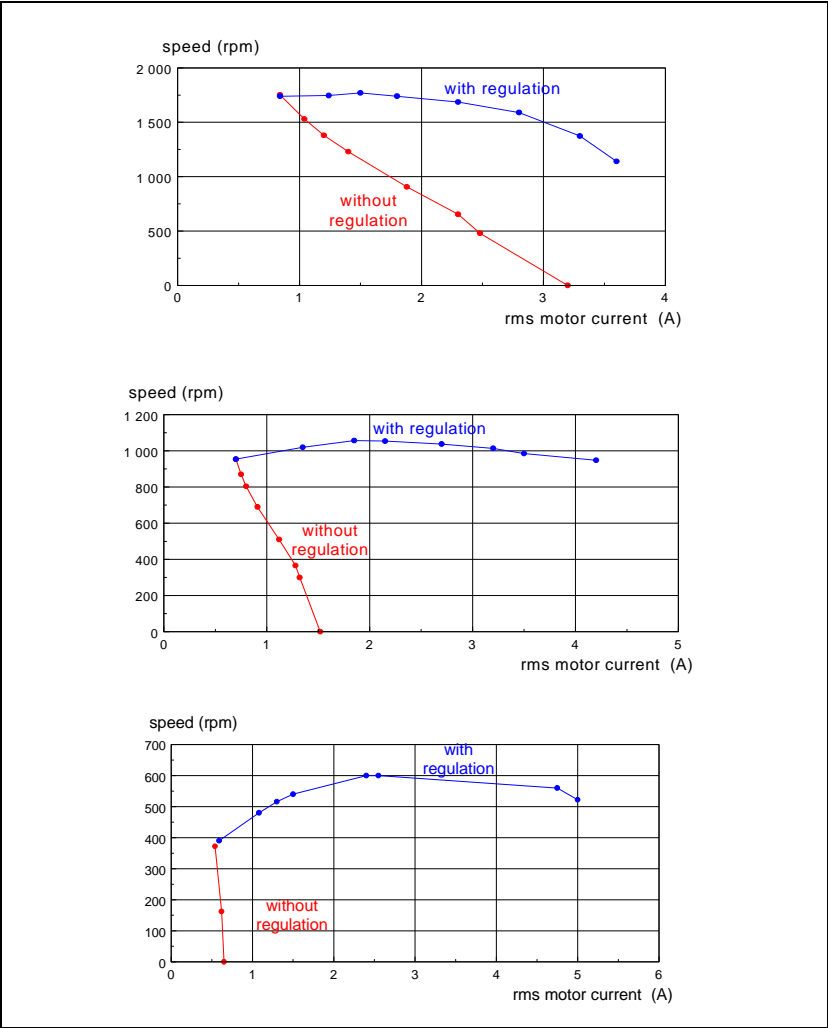
5 REGULATION PERFORMANCE

Figures 7, 8, 9 show the regulation performance at three speeds typical of a drill. The horizontal axis shows the motor rms current, which is proportional to the load. The first two figures show reasonable performance: speed is kept constant within $\pm 10\%$. The last figure, corresponding to a very low speed of 400 rpm, shows a speed increase when the load increases. This can be improved somewhat by fine tuning the compensation table. Creating a different table for each set speed would also improve the performance for a given set speed (for example, one table for set speeds 400-600 rpm, one for 600-900 rpm, one for 900-1300 rpm, etc... the example program provides only one table for the whole speed range). However, it should be noted that the difficulty to find the best compromises increases considerably when we want to regulate the motor at slower and slower speeds. This is easy to understand conceptually, as the quantity that we actually measure and regulate is $k.\Omega + r$. When we move towards slower speeds, the relative importance of the term $k.\Omega$ compared to the resistive term r becomes smaller and smaller. Also, at very low speeds, friction becomes predominant. This limits the usefulness of the system to moderate speed range applications.

6 CONCLUSION

This document showed how to regulate the universal motor speed without speed sensor, with the help of a low cost micro controller. The price to pay is some accuracy loss in the speed regulation, in the order of 10%. In most home appliance applications, such speed variation with varying load is fully acceptable. When the micro investment has been made, it is a good idea to make use of its inherent benefits, flexibility, ease of customization, fast time to market. In a washing machine for example, the micro can also be used to generate the speed ramps and washing / rinsing sequences, and control the unbalance; in a drill, it can be used to control or limit the torque. In the long term, the universal motor should be replaced more and more by brushless "electronic" motors, such as the DC permanent magnet brushless, or the switched reluctance motor, due to their higher efficiency and dynamic performances. However, cost reductions such as the one described in this document should allow the universal motor to compete successfully for many years in the most cost sensitive applications.

Figures 7, 8, 9. Speed regulation performance (with and without regulation) for set speeds of 1700, 950 and 400 rpm on a 500W drill. Speeds are measured after reduction, on the tool shaft



7 REFERENCES

- [1] Power control with triacs and ST6210 MCU
AN392 - P. Rabier and L. Perier (SGS-THOMSON Microelectronics)
- [2] Digital control for brush DC motor
T. Castagnet and J. Nicolai (SGS-THOMSON Microelectronics)
PCIM Nuremberg, June 93
- [3] Sensorless motor drive with the ST62 MCU + TRIAC
AN416 - T. Castagnet (SGS-THOMSON Microelectronics)

8 ANNEX

ANNEX 1 MOTOR CURRENT CALCULATION

The motor voltage equation is: $v(t) = (k.\Omega + r) i(t) + L di/dt$

$v(t) = 0$ while the triac is off (before turn on at time t_d , and after the turn off caused by the motor current reaching 0)

$v(t) = V_0 . \sin \omega t$ while the triac is on

The solution to the differential equation is:

$i(t) = 0$ while the triac is off

While the triac is on:

If we neglect the inductance L: $i(t) = V_0 \sin \omega t / (k.\Omega + r)$

If we do not neglect the inductance:

$i(t) = - \exp(-A(t-t_d)/L) [B \sin \omega t_d + C \cos \omega t_d] + B \sin \omega t + C \cos \omega t$

with: $A = k.\Omega + r$

$$B = AV_0 / (A^2 + L^2 \omega^2)$$

$$C = - L \omega V_0 / (A^2 + L^2 \omega^2)$$

t_d = triac firing delay measured from mains zero-crossing

Figure 10 is a plot of $i(t_0)$ versus t_d at constant speed. Modifying the speed parameter generates a family of curves. In Figure 11, t_0 equals 10 mS: the current $i(t_0)$ is measured at the mains voltage zero crossing.

Figure 11 is a plot of $i(t)$ versus t at constant speed. Modifying the parameter t_d (triac firing delay) generates a family of curves

Figure 10. calculated current versus time at constant speed for various triac firing delays (resistive and inductive model). Current at t_0 is constant, except at the largest firing delay t_d of 9 mS.

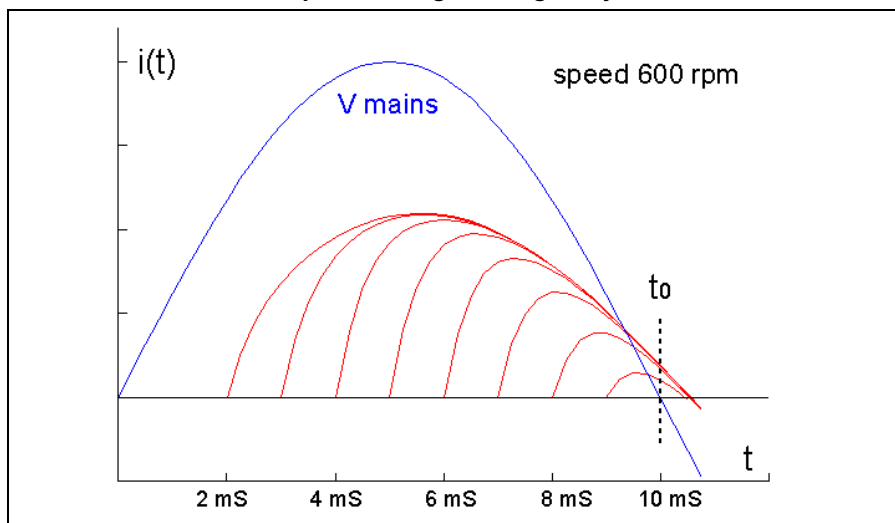
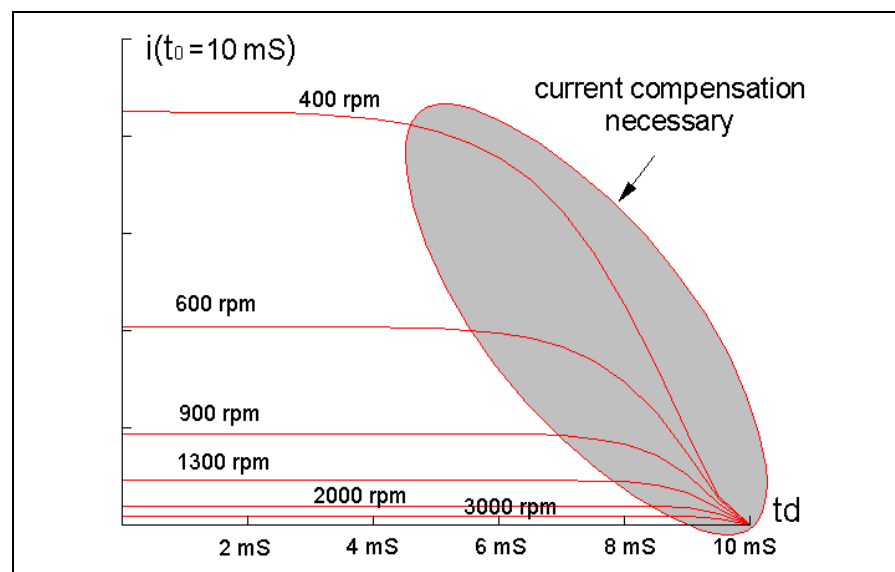


Figure 11. calculated current at mains zero crossing versus firing delay for various speeds. For speeds larger than 600 rpm and firing delays smaller than 7 mS, this current depends only upon speed.



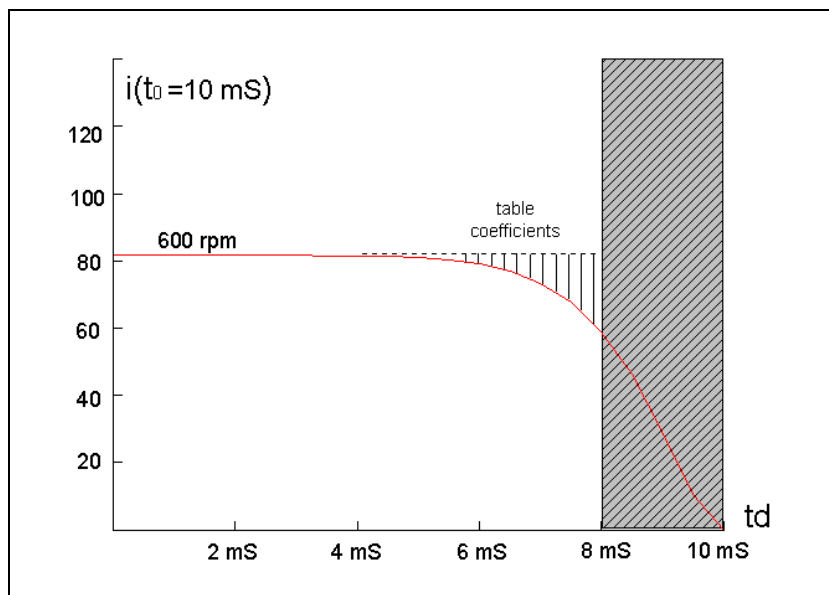
ANNEX 2 CREATING THE CURRENT COMPENSATION TABLE

A second assembly program is provided, named `caract.asm`. It must be used in place of “`regul.asm`”. Its purpose is to allow characterization of the motor in order to create the table. Contrary to “`regul.asm`”, it does not perform any regulation, but instead fires the triac at a constant delay t_d which can be adjusted through the whole range (VITMAX to VITMIN) by means of the two push buttons. At the same time, the RS232 connection allows to measure the present values for t_d (firing delay) and i_{t0} (measured current at zero crossing), as explained in annex 3. The procedure to follow is described below:

- select the desired speed for which the table must be optimized. Figure 12 gives an example (600 rpm) of the shape that current i_{t0} has while t_d is varied. This curve is in fact one of the curves family in Figure 12 of annex 1. This speed is obtained with no load by adjusting t_d with the push-buttons. The RS232 connection allows to measure and record t_d and i_{t0} when the desired speed is obtained.
- add a small constant load on the motor shaft. The speed naturally decreases. Then decrease the firing delay t_d with the push buttons until the speed is back to 600 rpm. At this time, record t_d and i_{t0} .
- increase slightly the load. Decrease t_d to come back to 600 rpm. Record again t_d and i_{t0} . Keep increasing the load until t_d reaches the minimum allowed, and record a few couples (t_d, i_{t0}).
- If you make a graph of the couples (t_d, i_{t0}) with t_d in abscissa, you will obtain a curve similar to the one in Figure 12. Subtracting the current value for small t_d , approximately 80 in Figure 12, will give the values for the look-up table: the table coefficients are zero for $t_d = 0$ to 4mS, then increase regularly up to approximately 22 for $t_d = 8$ mS. (note that, for the vertical axis, the values given are not amperes, but register values output by the ADC converter. They can be related to the actual current by taking account that the ADC value changes by one unit for 20 mV voltage change at its input PB1: when the input is maximum, 5 volts, the ADC value is 255). In the example of Figure 12, the table will look similar to the following:

t_d (mS)	0	1	2	3	4	5	5.5	6	6.5	7	7.5	8
coefficient	0	0	0	0	0	3	4	7	10	15	18	22

Figure 12. Variation of the current at zero-crossing $i(t_0)$ versus firing delay t_d at 600 rpm, while the load is varying. The cross-hatched area is not allowed, as friction keeps the motor stalled for very large firing delays. The set of vertical lines is a graphic representation of the table contents.



ANNEX 3 MONITORING ON A PC COMPUTER SCREEN

In order to monitor various variables during the motor characterization, an RS232 connection is provided in the micro-controller software between the ST6 and a personal computer. In the program “regul.asm”, two data bytes are sent to the PC every mains cycle: on negative half-cycles, the measured current *it0* is sent, and on positive half-cycles, the calculated firing delay *td* is sent. The instructions used to send this data are the following:

for the *it0* byte:

```
ld    a,it0
call  rs232
```

and for the *td* byte:

```
ld    a,td
call  rs232
```

When it is called, the *rs232* subroutine sends at 19200 bauds on port pin PA3 the data byte contained in the accumulator. This takes approximately 0.5 mS. Replacing *it0* or *td* by another register or RAM variable allows to send any intermediate calculation result or variable (coefficient from look-up table, proportional term, integral term, current error...). To connect the PA3 and VDD micro-controller pins to the PC require a level amplification (to boost the signal level from 0-5 volts to -5 / +5 volts) performed by a Maxim MAX232 circuit, and galvanic isolation, performed by an optocoupler (see Figure 13). The 9-pin connector must be connected to the COM1 serial port of the PC.

On the PC side, two executable programs are provided: NUMBER.EXE and VISU.EXE.

NUMBER.EXE, executed on the PC while the motor is running, displays on the screen two rows of data in decimal format representing the evolution in time of the received data *it0* and *td*. The two rows scroll down the screen, and at the same time are stored in a text file named NUMBER.PRN. Hitting any key stops the program execution. The data file NUMBER.PRN remains, available for latter use. It can be imported into a spreadsheet program for example, to visualize the curves representing in time domain the evolution of *it0* and *td*.

Program VISU.EXE, on the other hand, allow to display graphically in real time the time domain evolution of *it0* and *td*. The attached file EGAVGA.BGI must be present in the same directory, and the PC must have a VGA (or better) screen, as the graphic is displayed in 640x480 pixels resolution. Hitting any key (except “e”) stops temporarily the curves drawing, so the user can pause to examine a detail of the display.

9 REVISION HISTORY

Table 1. Revision history

Date	Revision	Description of changes
October 1996	1	Initial release
12-June-2008	2	Logo modified

Please Read Carefully:

Information in this document is provided solely in connection with ST products. STMicroelectronics NV and its subsidiaries ("ST") reserve the right to make changes, corrections, modifications or improvements, to this document, and the products and services described herein at any time, without notice.

All ST products are sold pursuant to ST's terms and conditions of sale.

Purchasers are solely responsible for the choice, selection and use of the ST products and services described herein, and ST assumes no liability whatsoever relating to the choice, selection or use of the ST products and services described herein.

No license, express or implied, by estoppel or otherwise, to any intellectual property rights is granted under this document. If any part of this document refers to any third party products or services it shall not be deemed a license grant by ST for the use of such third party products or services, or any intellectual property contained therein or considered as a warranty covering the use in any manner whatsoever of such third party products or services or any intellectual property contained therein.

UNLESS OTHERWISE SET FORTH IN ST'S TERMS AND CONDITIONS OF SALE ST DISCLAIMS ANY EXPRESS OR IMPLIED WARRANTY WITH RESPECT TO THE USE AND/OR SALE OF ST PRODUCTS INCLUDING WITHOUT LIMITATION IMPLIED WARRANTIES OF MERCHANTABILITY, FITNESS FOR A PARTICULAR PURPOSE (AND THEIR EQUIVALENTS UNDER THE LAWS OF ANY JURISDICTION), OR INFRINGEMENT OF ANY PATENT, COPYRIGHT OR OTHER INTELLECTUAL PROPERTY RIGHT.

UNLESS EXPRESSLY APPROVED IN WRITING BY AN AUTHORIZED ST REPRESENTATIVE, ST PRODUCTS ARE NOT RECOMMENDED, AUTHORIZED OR WARRANTED FOR USE IN MILITARY, AIR CRAFT, SPACE, LIFE SAVING, OR LIFE SUSTAINING APPLICATIONS, NOR IN PRODUCTS OR SYSTEMS WHERE FAILURE OR MALFUNCTION MAY RESULT IN PERSONAL INJURY, DEATH, OR SEVERE PROPERTY OR ENVIRONMENTAL DAMAGE. ST PRODUCTS WHICH ARE NOT SPECIFIED AS "AUTOMOTIVE GRADE" MAY ONLY BE USED IN AUTOMOTIVE APPLICATIONS AT USER'S OWN RISK.

Resale of ST products with provisions different from the statements and/or technical features set forth in this document shall immediately void any warranty granted by ST for the ST product or service described herein and shall not create or extend in any manner whatsoever, any liability of ST.

ST and the ST logo are trademarks or registered trademarks of ST in various countries.

Information in this document supersedes and replaces all information previously supplied.

The ST logo is a registered trademark of STMicroelectronics. All other names are the property of their respective owners.

© 2008 STMicroelectronics - All rights reserved

STMicroelectronics group of companies

Australia - Belgium - Brazil - Canada - China - Czech Republic - Finland - France - Germany - Hong Kong - India - Israel - Italy - Japan - Malaysia - Malta - Morocco - Singapore - Spain - Sweden - Switzerland - United Kingdom - United States of America

www.st.com